JACS
JOURNAL OF THE AMERICAN CHEMICAL SOCIETY

Article

pubs.acs.org/JACS

Bowl Inversion and Electronic Switching of Buckybowls on Gold

Shintaro Fujii,*[,†] Maxim Ziatdinov,[†,∥] Shuhei Higashibayashi,[‡] Hidehiro Sakurai,*[,§] and Manabu Kiguchi*[,†]

[†]Department of Chemistry, Graduate School of Science, Tokyo Institute of Technology, 2-12-1 W4-10 Ookayama, Meguro-ku, Tokyo 152-8511, Japan

[‡]Research Center of Integrative Molecular Systems, Institute for Molecular Science, Myodaiji, Okazaki 444-8787, Japan

[§]Division of Applied Chemistry, Graduate School of Engineering, Osaka University, 2-1 Yamada-oka, Suita, Osaka 565-0871, Japan

Supporting Information

ABSTRACT: Bowl-shaped π-conjugated compounds, or buckybowls, are a novel class of sp^2-hybridized nanocarbon materials. In contrast to tubular carbon nanotubes and ball-shaped fullerenes, the buckybowls feature structural flexibility. Bowl-to-bowl structural inversion is one of the unique properties of the buckybowls in solutions. Bowl inversion on a surface modifies the metal−molecule interactions through bistable switching between bowl-up and bowl-down states on the surface, which makes surface-adsorbed buckybowls a relevant model system for elucidation of the mechano-electronic properties of nanocarbon materials. Here, we report a combination of scanning tunneling microscopy (STM) measurements and ab initio atomistic simulations to identify the adlayer structure of the sumanene buckybowl on Au(111) and reveal its unique bowl inversion behavior. We demonstrate that the bowl inversion can be induced by approaching the STM tip toward the molecule. By tuning the local metal−molecule interaction using the STM tip, the sumanene buckybowl exhibits structural bistability with a switching rate that is two orders of magnitude faster than that of the stochastic inversion process.

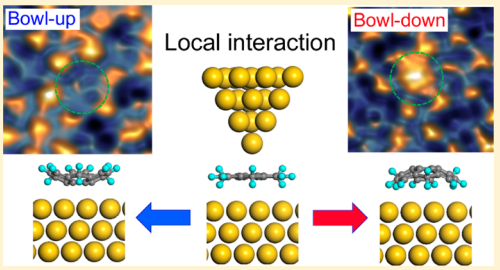

INTRODUCTION

The electronic properties of sp^2-hybridized carbon materials can be altered by tuning the degree of π-extension, shape, size, and edge geometry.[1−3] Bowl-shaped π-conjugated compounds are a novel class of sp^2-hybridized nanocarbon materials in addition to tubular carbon nanotubes and ball-shaped fullerenes. Bowl-shaped π-conjugated compounds,[4−6] such as corannulene and sumanene (Figure 1a), are referred to as buckybowls, because they can be considered as a fragment of a ball-shaped fullerene. The rich coordination chemistry of buckybowls such as corannulene and sumanene allows for stable adlayer-formation on metal surfaces, including Ag(111), Cu(111), and Cu(110),[7−11] which are important model systems for studying the electronic properties of metal−molecule interfaces relevant in molecular electronics. Buckybowls on metal surfaces acquire an additional structural degree of freedom with their bowl-up and bowl-down conformations due to inversion of the bowl-shaped carbon backbone. Bowl-to-bowl inversion is known as a characteristic behavior in solution. For example, sumanene exhibits bowl-to-bowl inversion with an inversion barrier of ca. 0.9 eV in solution.[12,13] The inversion barrier on Ag(111) has been predicted to be ca. 0.9 eV, based on a density functional theory (DFT) simulation;[7] however, the dynamic properties of bowl inversion on a surface remain to be solved.

Here, we demonstrate the facile adlayer preparation of sumanene buckybowls on Au(111) at room temperature, which is characterized using scanning probe microscopy (STM) under ultrahigh vacuum (UHV) conditions. The unique intrinsic properties of buckybowls on metal surfaces allow for a densely packed single layer of sumanene to readily self-organize to form a single adlayer from solution. The intrinsic curvature of the buckybowl results in bowl-up and bowl-down conformations on the substrate (Figure 1b), which makes it a promising research target for investigation of the operating principle of molecular switch or memory in the field of mechano-electronics. A combination of STM on the single molecule scale and DFT-based atomistic simulations reveals the unique dynamic bowl inversion behavior of sumanene on Au(111). The surface-adsorbed sumanene exhibits dynamic inversion that can be induced by external stimulus from an STM tip. This study demonstrates that the molecular self-assembly of buckybowls on metal surfaces provides a new class of π-systems on metals, which enables elucidation of the unique mechano-electronic properties evident at metal−molecule interfaces.

EXPERIMENTAL SECTION

STM experiments were performed with a commercially available STM (JEOL, JSPM-4500S) operated under ultrahigh vacuum at room temperature. Au(111) substrates were prepared by thermal evaporation of Au onto mica at 300 °C. All STM images were acquired in constant-current mode using mechanically cut Au wire as STM tips. The Au tip is used as a local electrode for the interaction with the surface-absorbed molecule at the closest approach in the bowl inversion experiment. Prior to STM characterization, the Au tips were heat-treated in an STM-

Received: May 8, 2016
Published: August 24, 2016

DOI: 10.1021/jacs.6b04741
J. Am. Chem. Soc. 2016, 138, 12142−12149

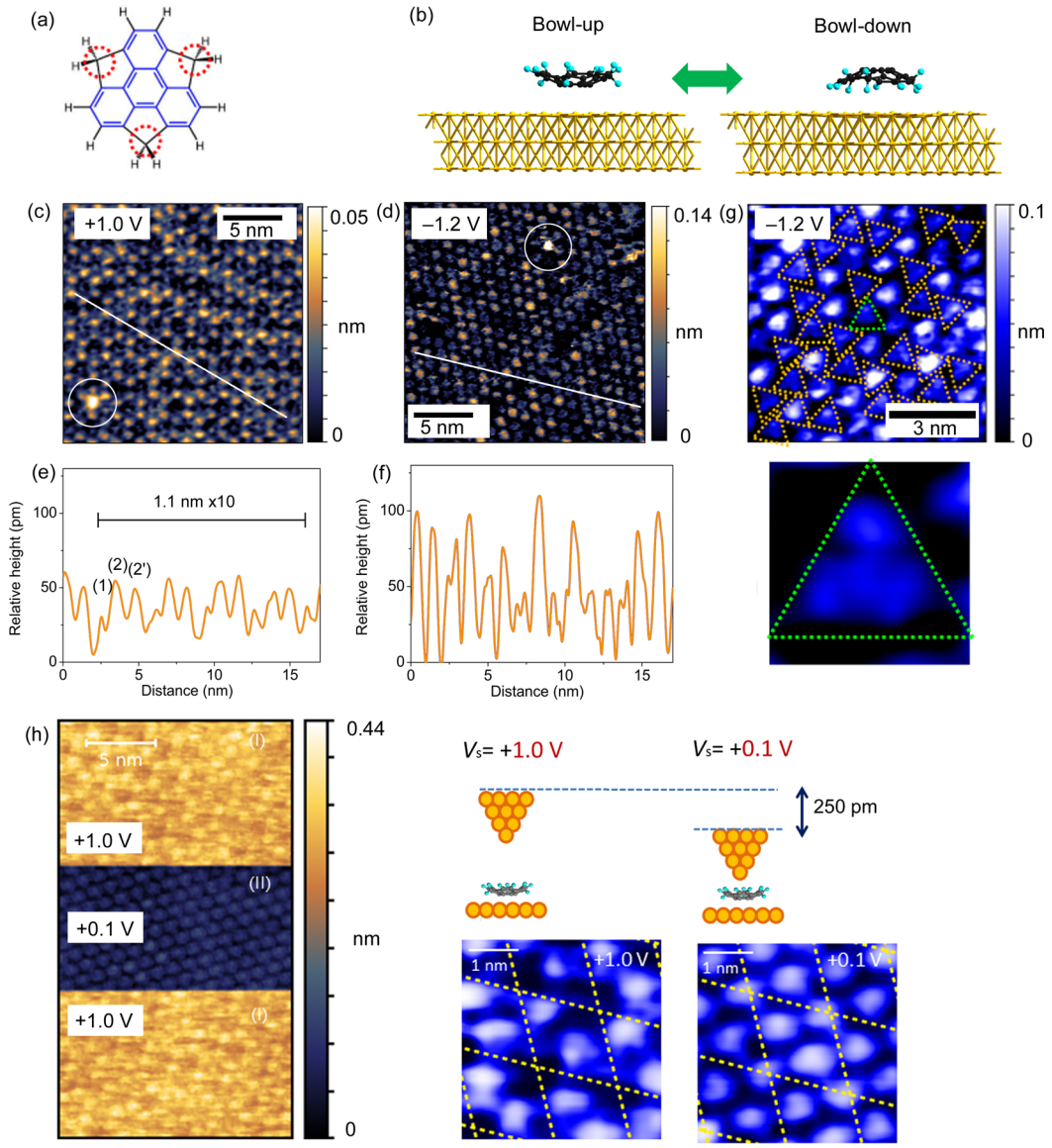

Figure 1. (a) Chemical structure of sumanene. Dihydrogenated carbon sites are marked by red circles. The sp^2-hybridized carbon backbone (i.e., triphenylene moiety) is indicated by blue bonds. (b) Schematic illustration of the bowl-up and bowl-down states for sumanene on Au(111), where gray, blue, and yellow balls correspond to C, H, and Au atoms, respectively. (c,d) Typical STM images with (c) honeycomb and (d) hexagonal patterns. Scale bars are 5 nm. Imaging conditions: (c) tunneling current (I_t) = 0.2 nA, sample bias voltage (V_s) = +1.0 V; and (d) I_t = 0.2 nA, V_s = −1.2 V. Exceptionally bright molecules are marked by circles, which are attributable to a molecule with a bowl-down conformation surrounded by a large number of molecules with a bowl-up conformation (for a detail, see main text). (e,f) Cross-sectional profiles along the lines in (c) and (d). The profile in (c) is characterized by periodic oscillation in heights with two peaks of (1), and (2) and (2′). The intermolecular spacing was measured to be ca. 1.1 nm by averaging 12 intermolecular spacing. (g) Magnified STM image of a hexagonal pattern. Molecules with clear triangular shapes are marked by dotted triangles. The triangular patterns are much more pronounced at a negative bias voltage. A magnified view of a triangular pattern located at the center in the STM image is shown at the bottom part. (h) STM image of sumanene adlayer on Au(111) imaged with different bias voltages of (i) 1.0 V and (ii) 0.1 V. The scale bar is 5 nm. The slow scanning direction was from up to down. To obtain the image, the bias voltage was changed while the tunneling current was held constant (0.1 nA). The bias voltage dependence of the STM patterns is reversible because the contrast reversibly changes from (i) to (ii) and back to (i). The inset shows magnified images of the areas of (i) and (ii) with dotted lines are overlaid as guides. The STM contrasts in (i) and (ii) are characterized by honeycomb and hexagonal patterns, respectively. As shown in the schematic illustration, the molecule−STM tip separation changed by 0.25 nm depending on the bias voltages, which can be seen as the relative change in the *z*-positions of the STM tip in the STM image.

treatment chamber at 150 °C for 12 h. Sumanene molecules[5] were deposited from a 10 mM solution toluene onto the Au(111) surface at room temperature for 20 min. DFT simulations of adsorption energies, equilibrium geometries, and inversion barriers were performed using CASTEP code[14] with/without van der Waals corrections.[15] Partial density of states (PDOSs) were summed for all C atoms and all H atoms. Inversion barriers were computed using the linear synchronous transit (LST) method[16] (see Supporting Information for further details). STM simulations were performed within the Tersoff−Haman approximation[17,18] using PWSCF code.[19]

RESULTS AND DISCUSSION

Adlayer Preparation and STM Characterization of Sumanene on Au(111). In most studies on the molecular deposition of nanocarbons onto metal surfaces, vacuum deposition methods have been successfully employed to prepare

DOI: 10.1021/jacs.6b04741
J. Am. Chem. Soc. 2016, 138, 12142−12149

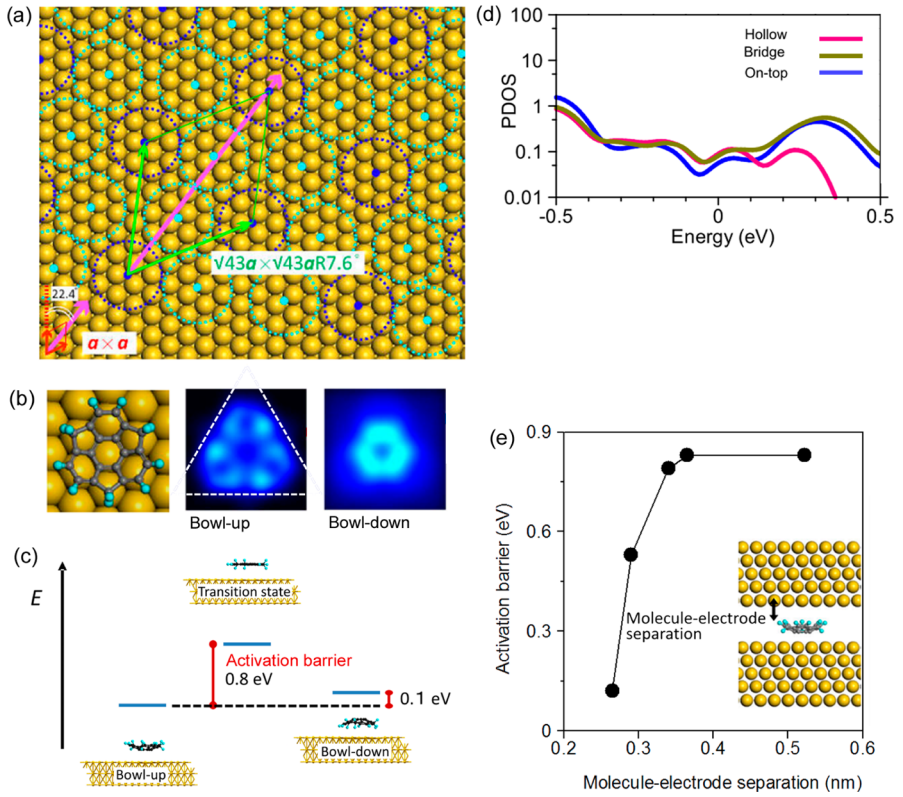

Figure 2. (a) Proposed adlayer structure of $(\sqrt{43} \times \sqrt{43})$R7.6° for sumanene on Au(111). Unit cell and vectors for Au(111) and the sumanene adlayer are represented by green and red lines, respectively. The pink arrow corresponds to the direction of a molecular row. The lattice vector of Au(111) is defined as ***a***. Sumanene molecules are represented by dotted circles, where blue and pale blue dotted circles, respectively, represent adsorbed on energetically favorable bridge and hollow sites on Au(111), respectively (see Figure S2). The nearest neighbor intermolecular distance is $(\sqrt{129})a/3$ = 1.09 nm. The rotational angle between an Au atomic row and a molecular row is 22.4° (=30° − 7.6°). (b) Simulated STM images at V_s = ± 0.5 V for bowl-up and bowl-down conformations. For the bowl-up conformation, the simulated images have almost identical patterns at negative and positive bias voltages. The triangular pattern is noticeable in the image, as is indicated by a dotted triangle. A structural model of the bowl-up conformation is shown on the left side. (c) Transition state representation of the bowl inversion process for an on-top adsorption model. (d) Dependence of the PDOSs of sumanene with the bowl-up conformation on the various adsorption sites. (e) Results of the transition state calculations of the bowl inversion process in the presence of another Au electrode (i.e., the STM-tip-electrode) on top of the molecule. Calculated activation barriers as a function of the molecule−electrode separation for three models. The molecule−electrode separation is defined as separation between a hydrogen atom at a dihydrogenated site of sumanene and a surface-Au atom in the top electrode.

well-ordered adlayers on metals. We determined that a simple solution-based deposition process is a promising method for the preparation of a well-ordered monolayer of buckybowls. Figure 1c−f shows typical STM images and cross-sectional profiles for a solution-processed sumanene-adlayer on Au(111) recorded at two different sample bias voltages of +1.0 and −1.2 V, in which periodic honeycomb and hexagonal patterns with a molecular spacing of ca. 1 nm are apparent for high and low bias voltage, respectively. The formation of a well-ordered monolayer implies substantial interaction between sumanene and the metal substrate as well as sufficient interactions among molecules (see also Figure S1).

In the periodic honeycomb and hexagonal patterns of the sumanene buckybowl on Au(111), an exceptionally bright spot is noticeable on a molecule (Figure 1c,d) and is associated with the structural degree of freedom corresponding to the bowl-up and bowl-down conformations, which is discussed in detail in later sections. Figure 1h shows the dependence of the STM-patterns on the bias voltage during the imaging process (see also Figure S2). The STM-patterns change reversibly from honeycomb to hexagonal and back to the honeycomb pattern, which suggests that the pattern change is purely of electronic origin. Bias voltage dependence of the STM-patterns revealed that the honeycomb and hexagonal patterns, respectively, appear at the high positive voltage (+1.0 V, Figure 1c) and the negative-to-low bias voltage (from −1.2 to +0.1 V, Figure 1d,g). It should be noted that there is a molecule at the dark central spot in the honeycomb pattern, although the molecule is invisible in the STM image, as demonstrated theoretically in a later section.

The hexagonal pattern (Figure 1d,g) with a molecular spacing of ca. 1 nm recorded at +0.1 V is similar to that observed for closely packed C_{60} on Au(111),[20−29] while the honeycomb pattern[7] at +1.0 V (Figure 1c) is a novel class of periodic patterns unique for the sumanene buckybowl. At negative bias voltage (V_s = −1.2 V), the hexagonal pattern has pronounced spatial variations in the individual molecular contrast (Figure 1g). Each molecule in the hexagonal pattern has a triangular shape, which reflects the spatial distribution of π-electrons in the carbon backbone (Figure 1a) and thus the molecular rotations.

Closer inspection of the STM height profiles (Figure 1e,f) and rotational angles of the molecular rows in the hexagonal lattice against the underlying Au(111) (Figure S3) revealed an intermolecular distance of 1.1 nm and a rotational angle of 22−23°, respectively. Following the procedure to find the most probable adlayer structures for spherical adsorbates on the Au(111) surface,[30] we propose a higher-order-commensurate

DOI: 10.1021/jacs.6b04741
J. Am. Chem. Soc. 2016, 138, 12142−12149

adlayer structure (Figure 2a) by taking into account both the observed intermolecular distance (1.1 nm) and the rotational angle (22−23°). In the higher-order-commensurate structure, molecules are sitting on either bridge or hollow sites of Au(111) to form a honeycomb pattern in terms of the adsorption sites (see also Figure S5). At first glance, the higher-order-commensurate structure looks too complicated to explain the observed simple hexagonal adlayer structure; however, the higher order commensurability is required to reproduce the observed honeycomb pattern with the unconventional bias dependence (Figure 1h).

Electronic Calculations and Identification of Sumanene-Adlayer Structure. As described in the Introduction, the buckybowls on surface acquire the additional structural degree of freedom that is the bowl-up and bowl-down conformations due to the inversion of the bowl-shaped carbon backbone (Figure 1b). To consider structural details for the observed hexagonal pattern, DFT simulations were performed using sumanene on Au(111)-slab models. Figure 2b−d and Figure S6 show DFT-simulated STM images, transition state of the bowl inversion, partial density of states (PDOSs), and total electronic energy. The electronic energy calculation revealed that the bowl-up conformation is energetically more stable than the bowl-down conformation by 0.1−0.8 eV, depending on the molecular orientations and adsorption sites (Figure S6). Transition state calculations confirmed an activation barrier of ca. 0.8 eV between the bowl-up and bowl-down states (Figure 2c), which acts as a substantial energy barrier to separate the two states. These results indicate that the sumanene adlayer consists almost entirely of a single phase with the energetically favorable bowl-up conformation at the ground state (Figure 1c,d,g). The simulated STM images (Figure 2b) reproduced the observed molecular contrast in the STM image (Figure 1g) and confirmed that the triangular-shape in the STM images corresponds to the molecular orientation.

The dependence of the rotational angles sumanene with bowl-up and bowl-down conformations on the electronic energy (Figure S6a) reveals that the total energy differs by less than 0.4 eV, which suggests that there is no preferential molecular rotational angle at room temperature. This is in good agreement with the experimental observation that the trianglar shape in a bowl-up molecule is oriented in several directions on Au(111) (Figure 1g). The PDOSs projected onto atomic orbitals of the molecule (Figure S6b) are weakly dependent on the molecular rotational angles, which appear in the cross-sectional STM profiles as small variations in heights (Figure 1f). Such variations in the STM profile height are strongly reminiscent of the C_{60}-adlayer structure on Au(111).[28,29] In a similar manner, the observation of randomly mixed bright and dim sumanene molecules (Figure 1f) is due to a difference in the molecular rotations. The PDOSs projected onto atomic orbitals of the molecules indicate a smaller DOS around the Fermi energy for the bowl-up conformation than for the bowl-down conformation (Figure S6c), which is a result of larger electronic stabilization due to a larger interaction between the molecular π-plane and the substrate for the bowl-up conformation.

In contrast to the molecular rotations, differences in molecular adsorption sites cause significant changes in the electronic structures of sumanene on Au(111) as shown in Figure S6c and Figure 2d. The total energy calculations (Figure S6c) reveal that molecular adsorption on the bridge and hollow sites is more energetically favorable than that on the on-top sites. The PDOSs for unoccupied states exhibit a strong dependence on the molecular adsorption sites (Figure 2d), in which the PDOSs disappear at the positive energies above ca. 0.15 V only for the hollow adsorption model. Therefore, at higher bias voltages, molecules on the hollow sites can be imaged as darker spots, while molecules on the bridge sites appear as brighter spots in an STM image. Consequently, the molecules on the energetically favorable hollow and bridge sites in the adlayer model (Figure 2a) are, respectively, imaged as darker and brighter in an STM image to form the honeycomb pattern at the higher bias voltage (Figure 1c; +1.0 V). In contrast, molecules on both of these adsorption sites (the hollow and bridge sites) are almost equally imaged as bright spots at the lower STM-bias voltage (Figure 1d,g; −1.2 and +0.1 V). The adsorption model presented in Figure 2a explains the unconventional STM-bias voltage dependence of the honeycomb pattern, in addition to the observed intermolecular distance and molecular orientation.

A very small fraction of molecules was determined to have pronounced heights in the observed STM images (see molecules marked by circles in Figure 1c,d). Molecules with an exceptionally large STM-height variation up to 100 pm (Figure S4) corresponded well with the enhanced local DOS (LDOSs) for the bowl-down conformation (Figure S6b). The combination of STM characterization and ab initio atomistic simulations revealed that the sumanene adlayer forms the higher-order-commensurate hexagonal lattice, in which the majority of the molecules are adapted to the bowl-up conformation with different molecular rotations with respect to the Au(111) lattice.

Effect of Local Interaction between the STM Tip and Sumanene on the Bowl Inversion Behavior. Following identification of the adlayer structure, we investigated the dynamic bowl inversion properties of the surface-adsorbed sumanene. The unique bowl-shaped structure of sumanene enables it to switch between two discrete states of bowl-up and bowl-down conformations (Figure 2c). To investigate the capability to induce the bowl inversion events by local interaction between a molecule and an Au-STM tip, transition state calculations of the bowl inversion process were performed in the presence of another Au electrode (i.e., an Au-electrode of the STM tip), which is placed on top of sumanene on Au(111) (Figure 2e). The activation barrier of the bowl inversion process was reduced along with approaching another Au-electrode (i.e., the Au-STM tip) to the surface-adsorbed sumanene molecule. At the closest approach on the atomic scale, the activation barrier is reduced drastically, which indicates that the local interaction between the STM-tip and sumanene can trigger the bowl inversion process by reducing the activation barrier. Using the calculated activation barriers of ca. 0.1 and 0.8 eV at the smallest and largest molecule−electrode separations, respectively, a reaction rate at the smallest separation is calculated to be ca. 3000 (i.e., exp(0.8/0.1)) times faster than that at the largest separation. The sumanene molecule at the transition state can be hybridized with the two Au electrodes at the small molecule−electrode separations (see inset in Figure 2e), which leads to reduction of the activation barrier through the interaction with the two Au electrodes and resulting energetic stabilization of the transition state. Besides the local interaction, tunneling-current could induce the bowl inversion event. For the electronic excitation of a surface adsorbed molecule, the existence of DOSs of an adsorbate near the Fermi energy is essential.[31,32] In the present sumanene/Au(111) system, the electronic excitation is less likely because the molecular PDOSs are sufficiently small (see Figure S7).

DOI: 10.1021/jacs.6b04741
J. Am. Chem. Soc. 2016, 138, 12142−12149

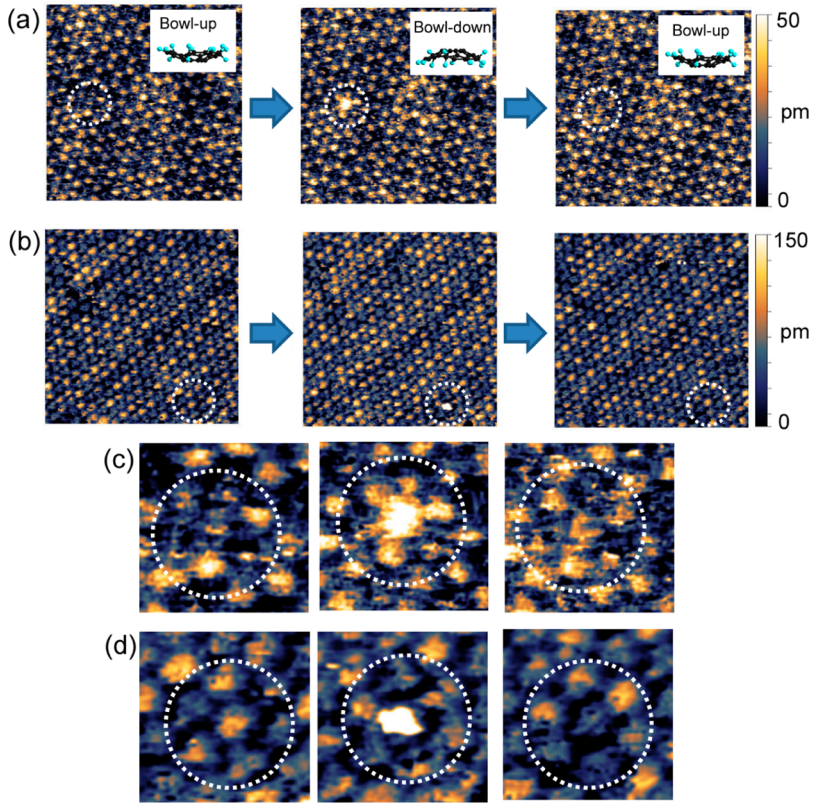

Figure 3. Reversible bowl inversions for sumanene on Au(111) at higher STM-bias voltages of (a) V_s = +1.0 V, (b) V_s = −1.2 V, with I_t = 0.2 nA for both (a) and (b). Imaging areas are 20 × 20 nm^2. A molecule subject to inversion events is marked by dotted circles. Schematic illustrations of the bowl-up and bowl-down conformations are shown at the right corners in the images. (c,d) Magnified images of sumanene with the bowl inversion events shown in (a) and (b), respectively.

A closer look at STM observations revealed that sumanene exhibited reversible bowl inversion process from up-to-down and down-to-up (Figure 3), which confirms the bistability of these two discrete states and suggests that the observed brighter spots are not due to contaminants from the surface and/or the tip but the molecule with the structural bistability. At a larger tip−molecule separation under the higher bias voltages (V_s = +1.0 V and −1.2 V), a small fraction of sumanene with the initial the bowl-up conformation exhibits bowl inversion behavior. At a large tip−molecule separation at V_s = +1.0 V (see Figure 1h), the stochastic inversion rate is estimated to be as high as 0.005 Hz (200 s), based on the lifetime of the bowl-up conformation in the sequence of the STM images (Figure 3a−d). It should be noted that the bowl inversion event was rarely observed and most of the molecules stayed intact in the bowl-up state with an inversion rate of almost zero under the high bias voltages at the large tip−molecule separation. At a small tip−molecule separation, a significant change in the bowl inversion behavior was observed, where sumanene begins to be subject to dynamic inversion between the bowl-up and bowl-down conformations (see also Supporting Information S8). The dependence of the bowl inversion behavior on the tip−molecule separations is in agreement with the results of the transition state calculations (Figure 2e). Figure 4a shows a higher resolution STM image recorded at a small tip−molecule separation (V_s = +0.1 V), in which sumanene with the bowl-up and bowl-down conformations is imaged as darker and brighter triangles, respectively. For the bowl-down conformation, a bright protrusion appears at the molecular center. These STM shapes and heights are in good agreement with DFT-simulated STM images (inset in Figure 4a). The dynamic inversion appears in the STM image as sudden changes in the STM-molecular height during the surface-scanning. Most of the observed bright spots (i.e., molecules with bowl-down conformation) exhibit the sudden changes in STM height, which is observed as scratches on the molecules during STM imaging. It should be noted that the scratches in the STM image can be due to scan line noises (instabilities) that come from a change in the STM-tip structure, unavoidable vibrational noise from the environment, and electronic noise from our instrument. Such instability-induced scratches can be distinguishable from the scratches due to the molecular bistability (i.e., the bowl inversion). The STM-induced bowl inversion appears as a scratch on a molecule, which is followed by the switch between bright and dark STM contrasts. In contrast, the instability-induced scratches can stochastically appear without the switch between bright and dark STM contrasts on a molecule; however, this was not the case in Figure 4a (see also Supporting Information S9).

Because the STM tip was raster-scanned above the molecules, the STM tip can locally interact with each molecule placed just below the STM tip during the scanning. Sumanene with the bowl-down conformation is characterized by a brighter protrusion at the molecular center (Figure 4b), while high frequency bowl inversion events between down and up conformations lead to bright and dark STM heights within the molecule (Figure 4c). The high frequency inversions are easily observed in the height profiles (Figure 4d). The STM height of the bowl-down state transits to the bowl-up state on the way of the STM-scanning and then switches back to the bowl-down state. It should be noted here that the transition was initiated

DOI: 10.1021/jacs.6b04741
J. Am. Chem. Soc. 2016, 138, 12142−12149

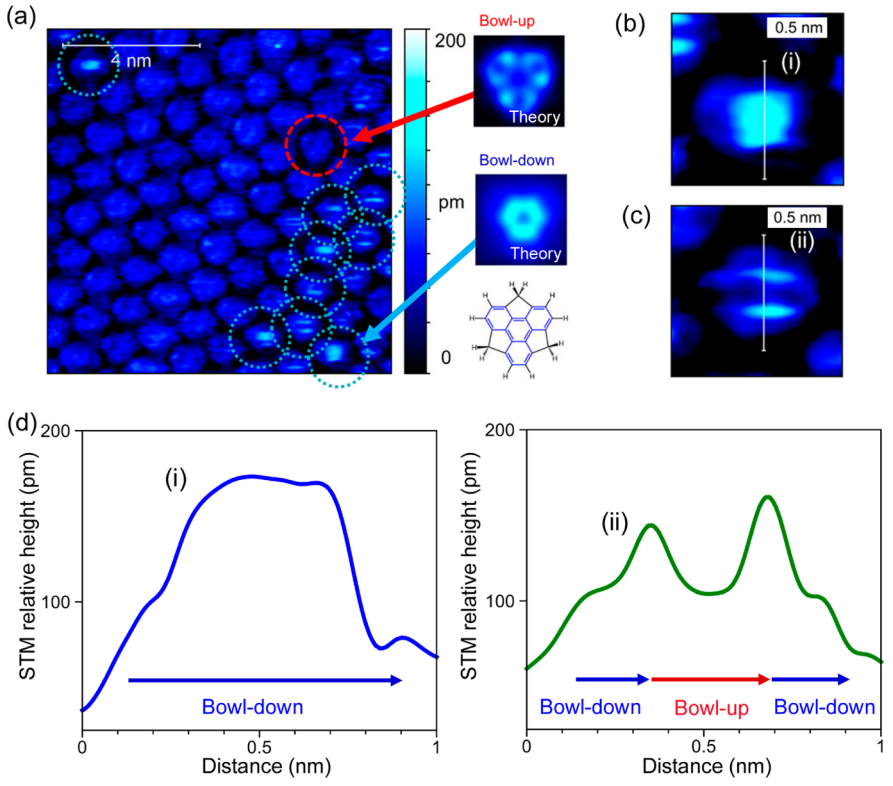

Figure 4. (a) High-resolution STM image recorded at a small tip−molecule separation under a low STM-bias voltage. The scale bar is 4 nm. Imaging conditions: V_s = +0.1 V, I_t = 0.9 nA. Red and blue circles correspond to molecules with the bowl-up and bowl-down conformations. The upper insets show DFT-simulated STM images for the bowl-up and bowl-down conformations at an STM-bias voltage of +0.5 V. The lower inset shows the molecular orientation used for the simulations. (b) Magnified images of molecules with the bowl-down conformation in (a). (c) Magnified images of the molecules with dynamic bowl inversion event during the imaging in (a). The initial bowl-down state switches to the bowl-up state, and then back to the bowl-down state. For details, see the main text. (d) Cross-sectional profiles measured on the lines indicated by (i) and (ii) in (b) and (c). For further details, see Supporting Information S9.

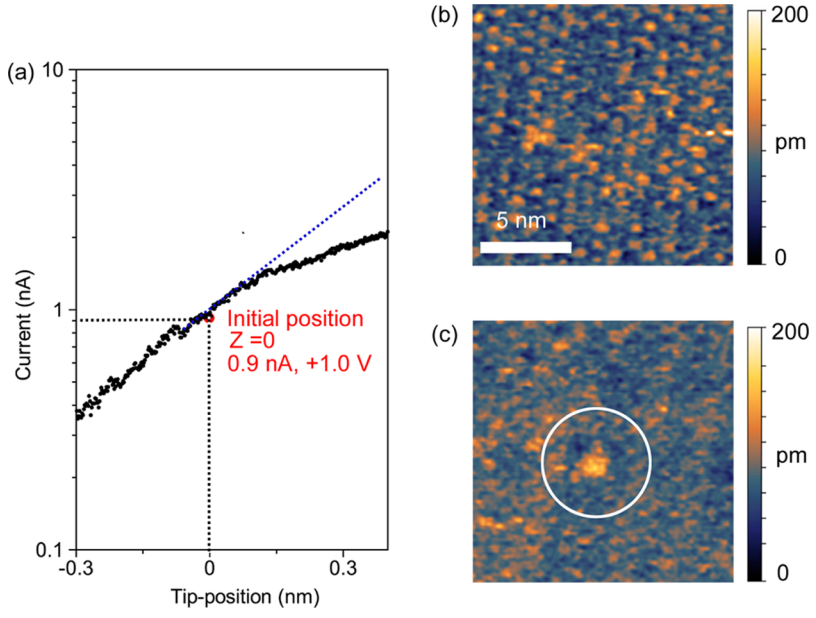

Figure 5. (a) Current versus distance curve during the manipulation process where the STM tip approaches a target molecule. The initial tip position is indicated by the red spot. A change is observed in the slope of the current versus distance curve. (b,c) STM images before and after the manipulation process. Imaging conditions: V_s = +1.0 V. I_t = 0.9 nA, imaging area = 15 × 15 nm^2. The manipulation process was performed on the center position of the image in (b). After the manipulation, the molecule with the bowl-up state transitioned to the bowl-down state, which appears as a bright protrusion (see dotted circle in (c)).

DOI: 10.1021/jacs.6b04741
J. Am. Chem. Soc. 2016, 138, 12142−12149

when the Au-STM tip scans across the molecule. This result indicates that the STM tip-induced local interaction on the molecule triggers the bowl inversions. The STM tip was found to approach the sumanene molecules at a distance of 250 pm (see the relative change in the z-positions of the STM tip with respect to the high (V_s = +1.0 V) and low (V_s = +0.1 V) bias voltages (Figure 1h)). At the closest approach of the Au-STM tip with the low bias voltage, sumanene can adsorb to either the surfaces of the Au-tip or the Au-substrate surface with the reduced activation barrier (Figure 2e) to form the energetically stable bowl-up state. By tuning the local metal−molecule interaction using the STM tip, the dynamic bowl inversion properties of sumanene can be modulated on the molecular scale. On the basis of the time required to transit from the bowl-down to the bowl-up states, and vice versa, during STM imaging (Figure 4), the inversion rate is calculated to be 0.3 and 0.5 Hz for down-to-up and up-to-down transitions, respectively. These rates are at least 2 orders of magnitude faster than the stochastic inversion rate of 0.005 Hz.

Finally, we demonstrate the manipulation of a bowl inversion event on a single molecule level using point contacts between an STM tip and a sumanene molecule. The STM tip is intentionally moved toward a target molecule on Au(111) at a fixed bias voltage (V_s = +1.0 V) to modulate the molecule−tip interaction that induces bowl inversion. During the manipulation process, where the STM tip is gradually moved toward the target molecule, the STM-feedback loop is opened and the tunneling currents are monitored. The current initially increased exponentially as a function of the tip−molecule distance (z-position) (Figure 5a), and the slope of the current versus distance curve suddenly changed at z = +0.15 nm. This change in slope can be interpreted as the effective contact of the tip with the top of the molecule, as reported previously.[33] The change in the slope suggests that a non-negligible local tip−molecule interaction occurs, which triggers the local bowl inversion event on the single molecule level. Figure 5b,c shows STM images before and after the manipulation process, respectively. Initially, all of the molecules are adsorbed on Au(111) with the bowl-up state (Figure 5b), while the STM height of the target molecule changes from a darker spot to a bright protrusion (see the dotted circle in Figure 5c) upon mechanical stimulus. Thus, the intentional introduction of a local mechanical perturbation enables the manipulation of a molecule from the bowl-up state to the bowl-down state (see also Supporting Information S10 and S11). The structural switch of the surface adsorbed sumanene provides new insight into the operating principle of mechano-electronic switch and memory in energy-saving electronic devices.

CONCLUSION

We have demonstrated the facile preparation of a sumanene buckybowl adlayer on Au(111) at room temperature. A combination of characterization using UHV-STM and ab initio electronic calculations has revealed that sumanene with the bowl-up conformation forms a well-ordered closely packed monolayer on Au(111), that is, $(\sqrt{43} \times \sqrt{43})$R7.6°. The dynamic bowl inversion properties can be modulated by tuning the local metal−molecule interaction using the STM tip. Under a weak tip−molecule interaction at a larger tip−molecule distance, sumanene exhibits stochastic inversion with a considerably slow rate of <0.005 Hz. In contrast, under a large tip−molecule interaction regime, sumanene exhibits structural bistability and dynamic switching between the bowl-up and bowl-down states that is 2 orders of magnitude faster. The molecular self-assembly of buckybowls provides a new class of π-systems on metals, which has enabled elucidation of their unique mechano-electronic properties at metal−molecule interfaces.

ASSOCIATED CONTENT

Supporting Information

The Supporting Information is available free of charge on the ACS Publications website at DOI: 10.1021/jacs.6b04741.

High-resolution STM images of C_{60} and buckybowl, STM patterns for sumanene adlayer imaged with different sample bias, rotational angles, cross-sectional profiles of STM patterns for sumanene adlayer, possible sumanene-adlayer models, DFT calculations of sumanene-adlayer with different rotational angles and different adsorption sites on Au(111), DOS calculations for sumanene on Au(111) and Pt(111), a set of three sequential images recorded at the low STM-bias condition, STM image corrections, additional point contact experiments, cross-sectional profiles on a molecule in the stochastic bowl inversion event and the point contact experiment, and details of DFT calculations (PDF)

AUTHOR INFORMATION

Corresponding Authors

*fujii.s.af@m.titech.ac.jp
*hsakurai@chem.eng.osaka-u.ac.jp
*kiguti@chem.titech.ac.jp

Present Address

[‖]Center for Nanophase Materials Sciences, Oak Ridge National Laboratory, Oak Ridge, Tennessee 37831, United States.

Notes

The authors declare no competing financial interest.

ACKNOWLEDGMENTS

This work was financially supported by Grants-in-Aid for Scientific Research in Innovative Areas (nos. 26102013, 2511008, 26102002) and Grants-in-Aid for Scientific Research (A) (no. 21340074), (B) (no. 26288020), and (C) (no. 25410124) from the Ministry of Education, Culture, Sports, Science and Technology (MEXT) of Japan, and ACT-C from the Japan Science and Technology Agency (JST).

REFERENCES

(1) Narita, A.; Wang, X. Y.; Feng, X.; Mullen, K. *Chem. Soc. Rev.* **2015**, *44*, 6616−6643.
(2) Ozaki, K.; Kawasumi, K.; Shibata, M.; Ito, H.; Itami, K. *Nat. Commun.* **2015**, *6*, 6251.
(3) Morita, Y.; Suzuki, S.; Sato, K.; Takui, T. *Nat. Chem.* **2011**, *3*, 197−204.
(4) Scott, L. T.; Hashemi, M. M.; Meyer, D. T.; Warren, H. B. *J. Am. Chem. Soc.* **1991**, *113*, 7082−7084.
(5) Sakurai, H.; Daiko, T.; Hirao, T. *Science* **2003**, *301*, 1878.
(6) Tsefrikas, V. M.; Scott, L. T. *Chem. Rev.* **2006**, *106*, 4868−4884.
(7) Jaafar, R.; Pignedoli, C. A.; Bussi, G.; Ait-Mansour, K.; Groening, O.; Amaya, T.; Hirao, T.; Fasel, R.; Ruffieux, P. *J. Am. Chem. Soc.* **2014**, *136*, 13666−13671.
(8) Bauert, T.; Baldridge, K. K.; Siegel, J. S.; Ernst, K. H. *Chem. Commun.* **2011**, *47*, 7995−7997.
(9) Merz, L.; Parschau, M.; Zoppi, L.; Baldridge, K. K.; Siegel, J. S.; Ernst, K.-H. *Angew. Chem., Int. Ed.* **2009**, *48*, 1966−1969.
(10) Xiao, W.; Passerone, D.; Ruffieux, P.; Ait-Mansour, K.; Groning, O.; Tosatti, E.; Siegel, J. S.; Fasel, R. *J. Am. Chem. Soc.* **2008**, *130*, 4767−4771.

DOI: 10.1021/jacs.6b04741
J. Am. Chem. Soc. 2016, 138, 12142−12149

(11) Parschau, M.; Fasel, R.; Ernst, K. H.; Groning, O.; Brandenberger, L.; Schillinger, R.; Greber, T.; Seitsonen, A. P.; Wu, Y. T.; Siegel, J. S. *Angew. Chem., Int. Ed.* **2007**, *46*, 8258−8261.
(12) Amaya, T.; Sakane, H.; Muneishi, T.; Hirao, T. *Chem. Commun.* **2008**, 765−767.
(13) Shrestha Binod, B.; Karanjit, S.; Higashibayashi, S.; Sakurai, H. *Pure Appl. Chem.* **2014**, *86*, 747−753.
(14) Segall, M. D.; Lindan, P. J. D.; Probert, M. J.; Pickard, C. J.; Hasnip, P. J.; Clark, S. J.; Payne, M. C. *J. Phys.: Condens. Matter* **2002**, *14*, 2717−2744.
(15) Tkatchenko, A.; Scheffler, M. *Phys. Rev. Lett.* **2009**, *102*, 073005.
(16) Govind, N.; Petersen, M.; Fitzgerald, G.; King-Smith, D.; Andzelm, J. *Comput. Mater. Sci.* **2003**, *28*, 250−258.
(17) Tersoff, J.; Hamann, D. R. *Phys. Rev. Lett.* **1983**, *50*, 1998−2001.
(18) Tersoff, J.; Hamann, D. R. *Phys. Rev. B: Condens. Matter Mater. Phys.* **1985**, *31*, 805−813.
(19) Paolo, G.; Stefano, B.; Nicola, B.; Matteo, C.; Roberto, C.; Carlo, C.; Davide, C.; Guido, L. C.; Matteo, C.; Ismaila, D.; Andrea Dal, C.; Stefano de, G.; Stefano, F.; Guido, F.; Ralph, G.; Uwe, G.; Christos, G.; Anton, K.; Michele, L.; Layla, M.-S.; Nicola, M.; Francesco, M.; Riccardo, M.; Stefano, P.; Alfredo, P.; Lorenzo, P.; Carlo, S.; Sandro, S.; Gabriele, S.; Ari, P. S.; Alexander, S.; Paolo, U.; Renata, M. W. *J. Phys.: Condens. Matter* **2009**, *21*, 395502.
(20) Altman, E. I.; Colton, R. J. *Surf. Sci.* **1992**, *279*, 49−67.
(21) Altman, E. I.; Colton, R. J. *Surf. Sci.* **1993**, *295*, 13−33.
(22) Altman, E. I.; Colton, R. J. *Phys. Rev. B: Condens. Matter Mater. Phys.* **1993**, *48*, 18244−18249.
(23) Hou, J. G.; Jinlong, Y.; Haiqian, W.; Qunxiang, L.; Changgan, Z.; Lanfeng, Y.; Bing, W.; Chen, D. M.; Qingshi, Z. *Nature* **2001**, *409*, 304−305.
(24) Wang, H.; Zeng, C.; Wang, B.; Hou, J. G.; Li, Q.; Yang, J. *Phys. Rev. B* **2001**, *63*.
(25) Sakurai, T.; Wang, X. D.; Xue, Q. K.; Hasegawa, Y.; Hashizume, T.; Shinohara, H. *Prog. Surf. Sci.* **1996**, *51*, 263−408.
(26) Gardener, J. A.; Briggs, G. A. D.; Castell, M. R. *Phys. Rev. B* **2009**, *80*.
(27) Tang, L.; Xie, Y.; Guo, Q. *J. Chem. Phys.* **2011**, *135*, 114702.
(28) Shi, X.-Q.; Van Hove, M. A.; Zhang, R.-Q. *J. Mater. Sci.* **2012**, *47*, 7341−7355.
(29) Passens, M.; Waser, R.; Karthauser, S. *Beilstein J. Nanotechnol.* **2015**, *6*, 1421−1431.
(30) Fujii, S.; Akiba, U.; Fujihira, M. *J. Am. Chem. Soc.* **2002**, *124*, 13629−13635.
(31) Ohara, M.; Kim, Y.; Yanagisawa, S.; Morikawa, Y.; Kawai, M. *Phys. Rev. Lett.* **2008**, *100*, 136104.
(32) Shin, H. J.; Jung, J.; Motobayashi, K.; Yanagisawa, S.; Morikawa, Y.; Kim, Y.; Kawai, M. *Nat. Mater.* **2010**, *9*, 442−447.
(33) Wakamatsu, S.; Fujii, S.; Akiba, U.; Fujihara, M. *Jpn. J. Appl. Phys.* **2006**, *45*, 2736−2742.

DOI: 10.1021/jacs.6b04741
J. Am. Chem. Soc. 2016, 138, 12142−12149